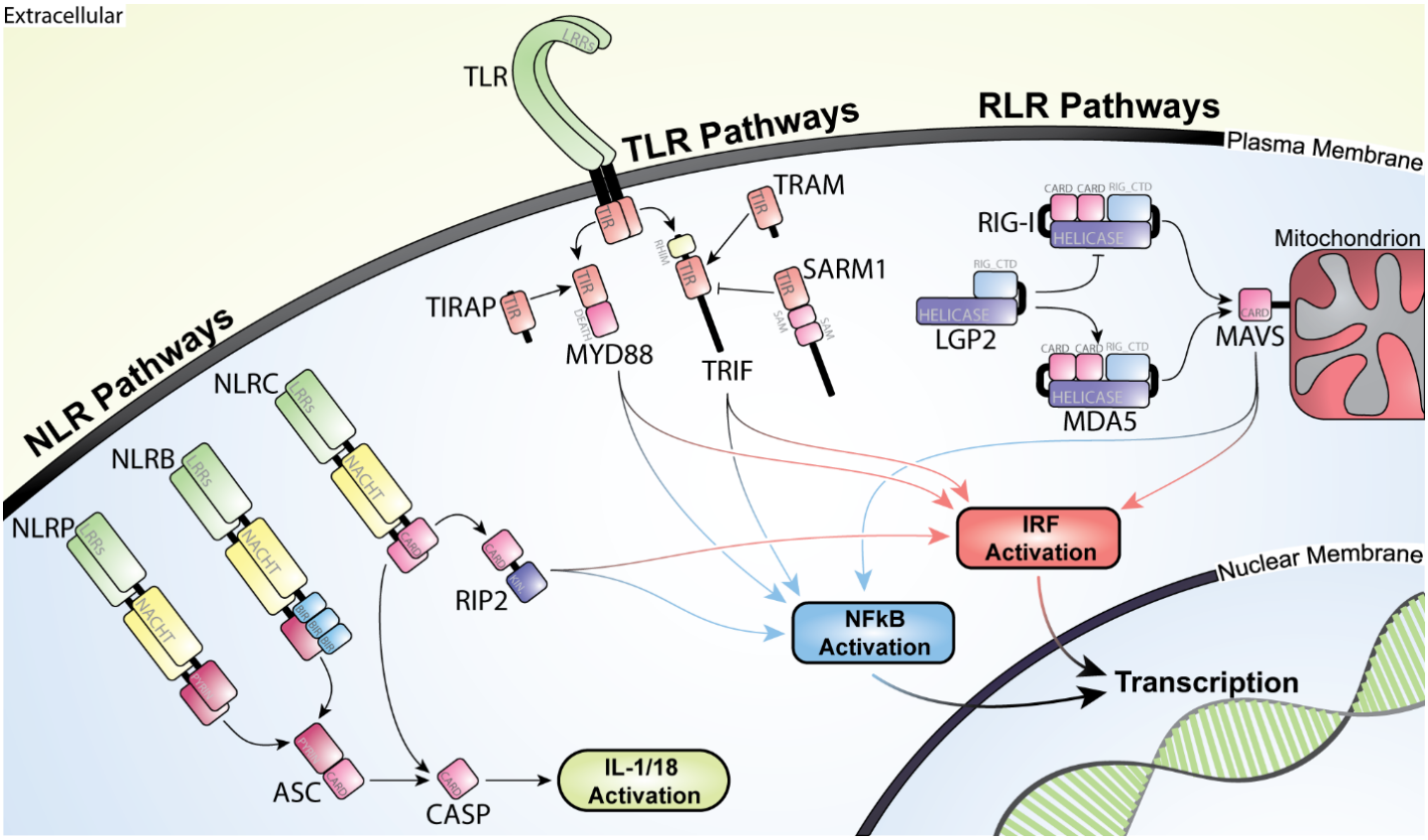

Supplementary Fig 1. Diagram of NLR, TLR, and RLR signaling pathways with all domains labeled. (Left) NLRs are cytoplasmically localized and possess a C-terminal series of leucine-rich repeats responsible for ligand binding, and a central NACHT domain involved in oligomerization and activation (Lechtenberg et al. 2014). NLR subfamilies differ in their N-terminal domain(s) which promote transcription factor activation or inflammasome assembly (Meunier & Broz, 2017). (Middle) TLRs are type-I transmembrane proteins localized to cell or endosomal membranes. Their N-terminal leucine-rich repeats bind pathogen-associated moieties, and the C-terminal TIR domain undergoes homotypic TIR domain interactions with one of five TIR-domain-containing adaptor proteins (Akira & Takeda 2004). (Right) RLRs are cytoplasmically localized and are exclusively involved in nucleic acid sensing. The central helicase and C-terminal regulatory domain are involved in ligand binding and autoregulation, whereas the N-terminal CARD domains are involved in signal transduction (Reikine et al. 2014). All three pathways converge on the activation of NF-κB and IRF activation, transcription factors which promote the expression of host-defense compounds like pro-inflammatory cytokines and antiviral peptides, respectively.

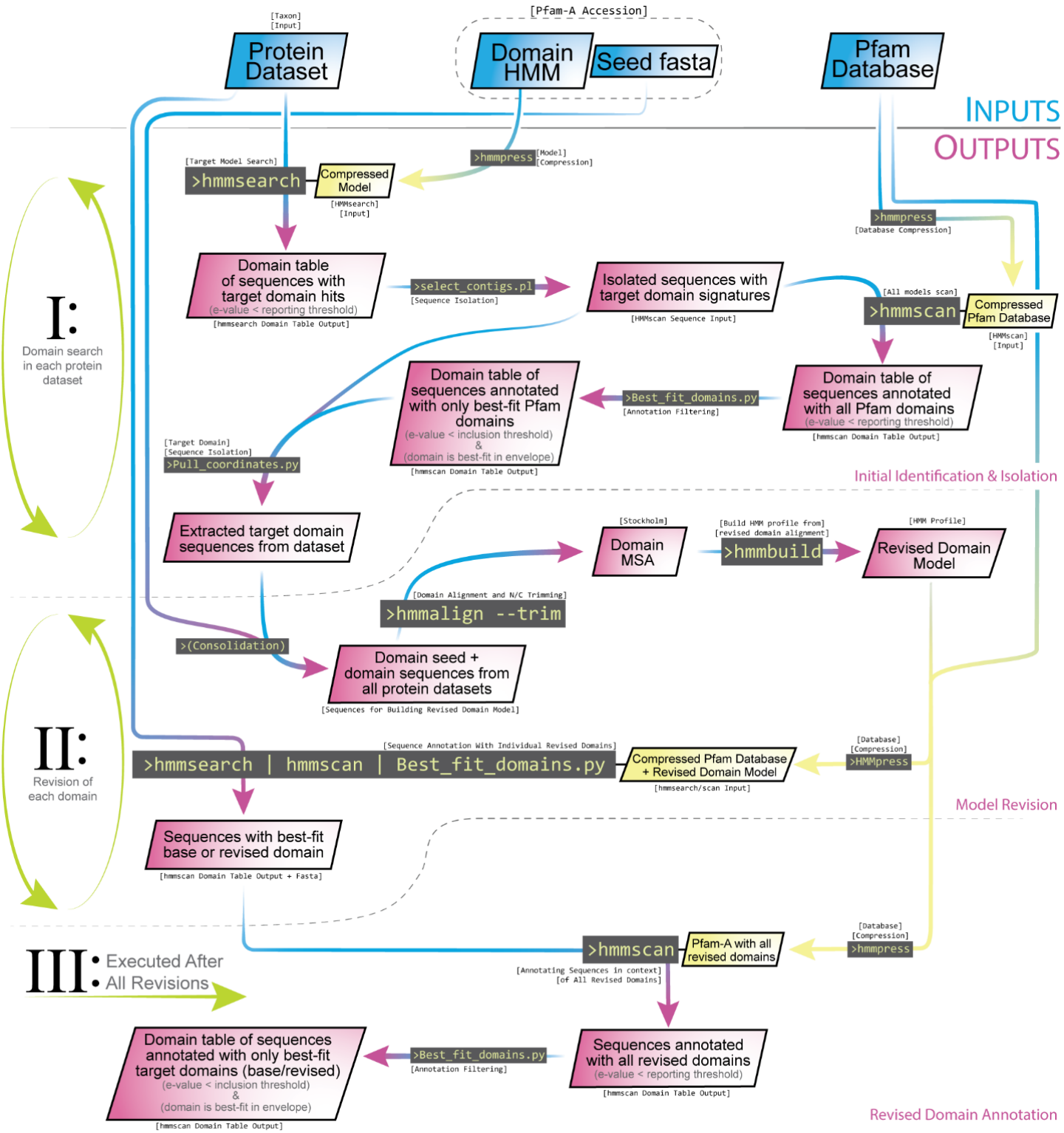

Supplementary Fig 2. Detailed schematic of commands and data analysis performed by TIAMMAt (see **Materials & Methods** for further detail).

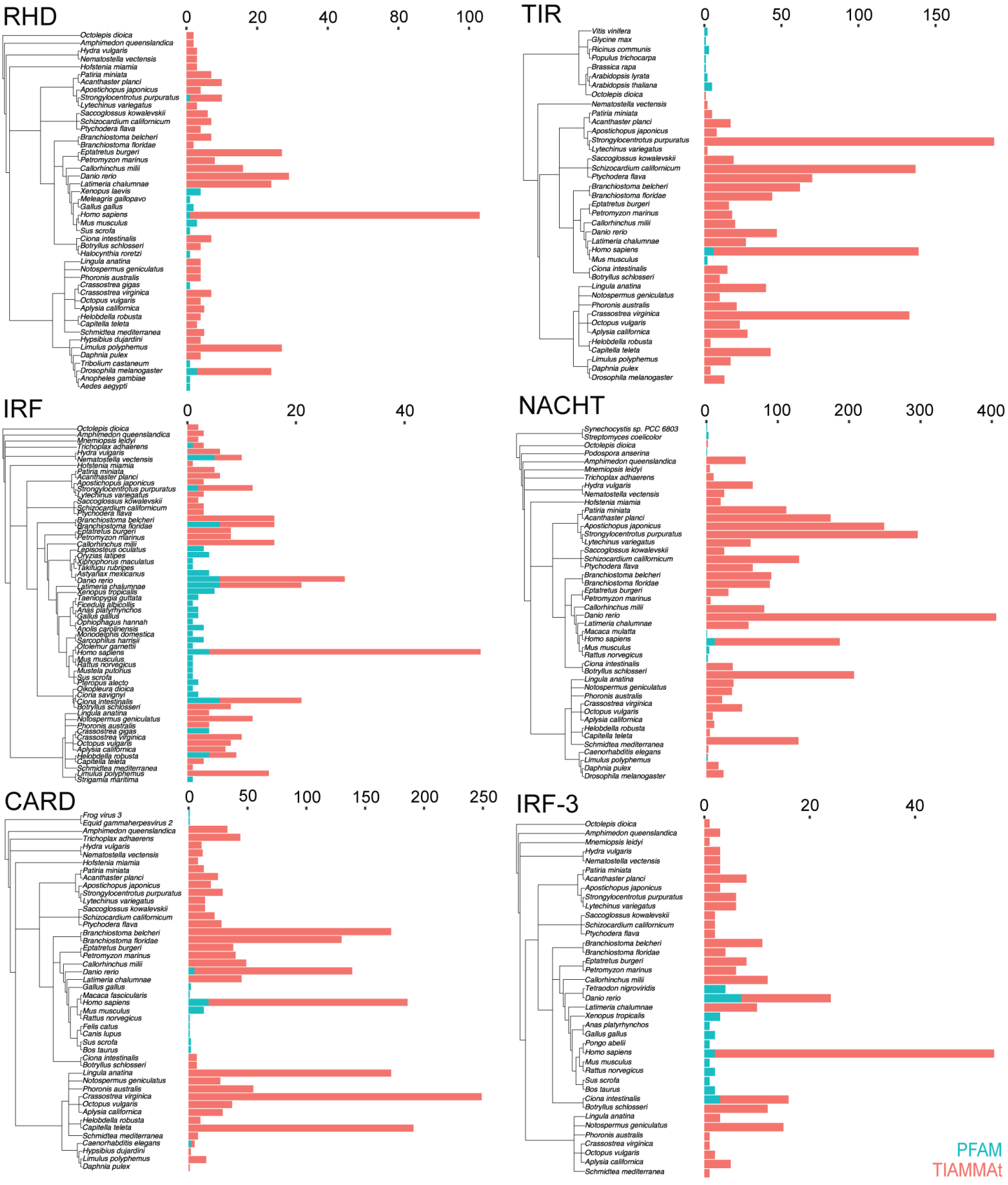

Supplementary Fig 3. Bar plots showing the number of sequences per species represented in domain seeds of RHD, TIR, IRF, NACHT, CARD, and IRF-3 before (blue) and after (red) domain revision by TIAMMAt. Blue and red bars are superimposed, and their scales are displayed above each individual plot. Phylogenetic relationships of species represented in each domain seed were derived of their NCBI taxonomy.

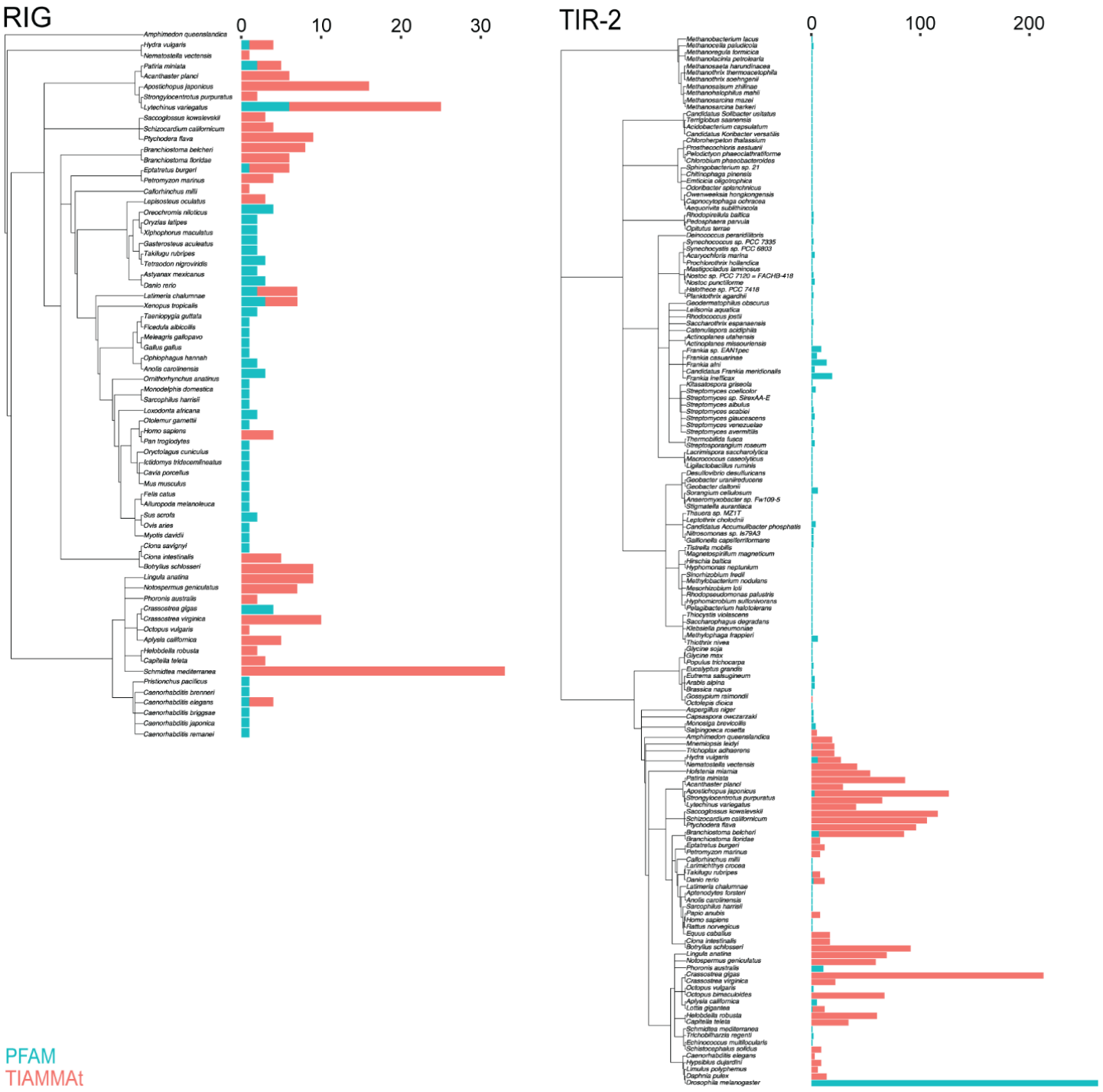

Supplementary Fig 4. Bar plots showing the number of sequences per species represented in domain seeds of RIG and TIR-2 before (blue) and after (red) domain revision by TIAMMAt. Blue and red bars are superimposed, and their scales are displayed above each individual plot. Phylogenetic relationships of species represented in each domain seed were derived of their NCBI taxonomy.

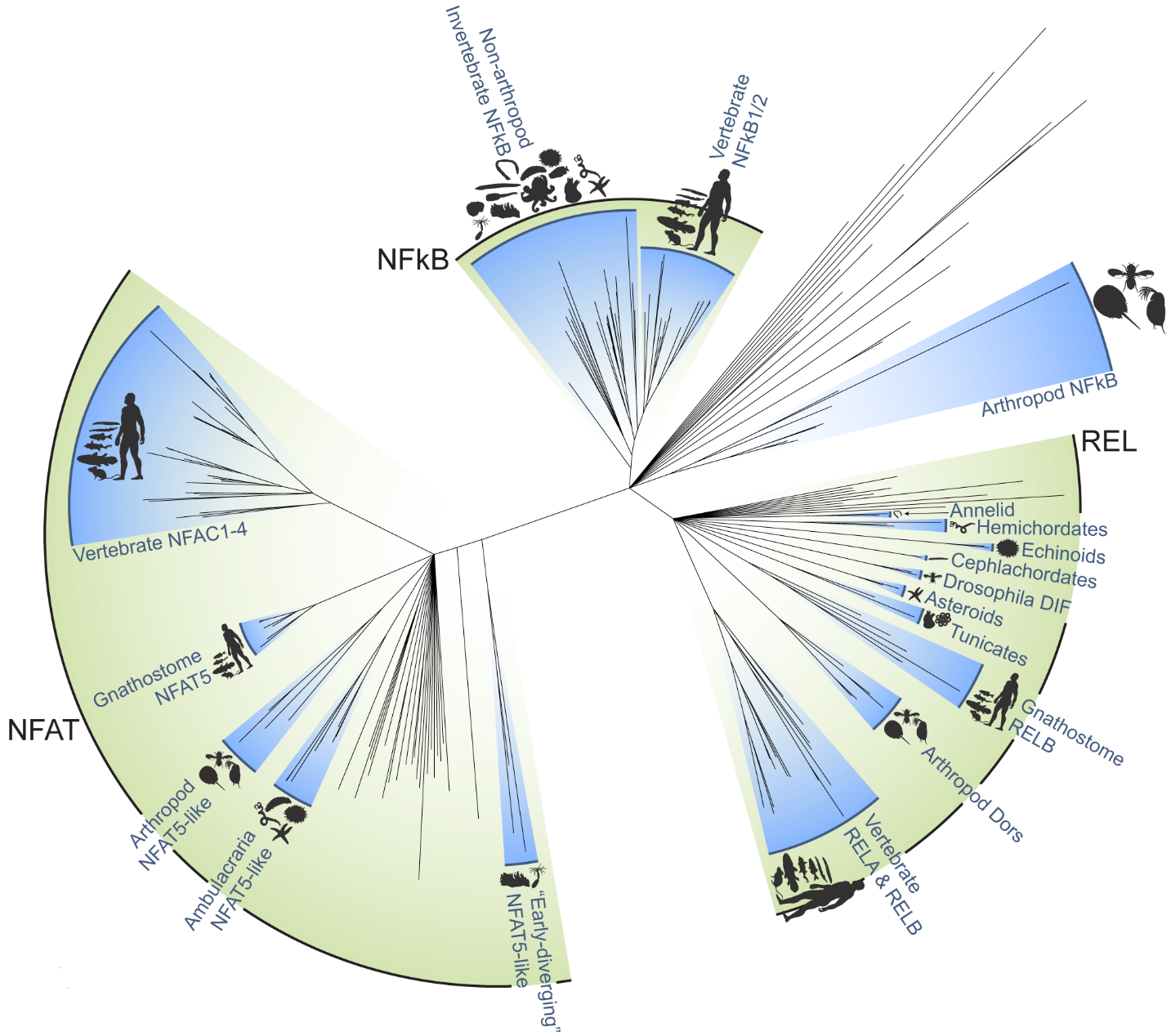

Supplementary Fig 5. Maximum-likelihood phylogenetic reconstruction of NF-κB family proteins using IQ-TREE. All nodes possess ultrafast-bootstrap support ≥95%. Best-fit model by BIC: VT+F+R6. Scale bar in number of substitutions per site.

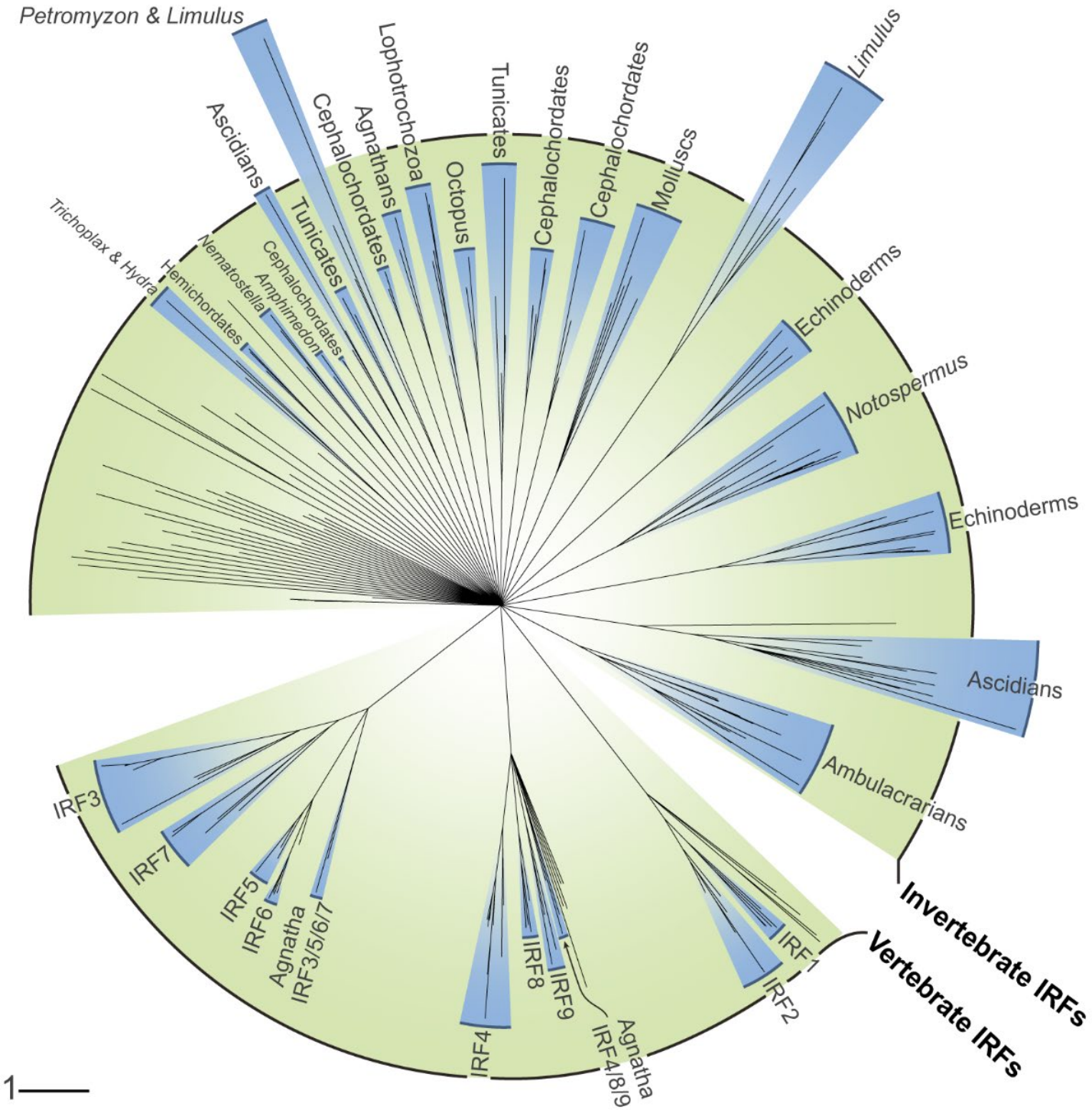

Supplementary Fig 6. Maximum-likelihood phylogenetic reconstruction of IRFs using IQ-TREE. All nodes possess ultrafast-bootstrap support ≥95%. Best-fit model by BIC: VT+R6. Scale bar in number of substitutions per site.

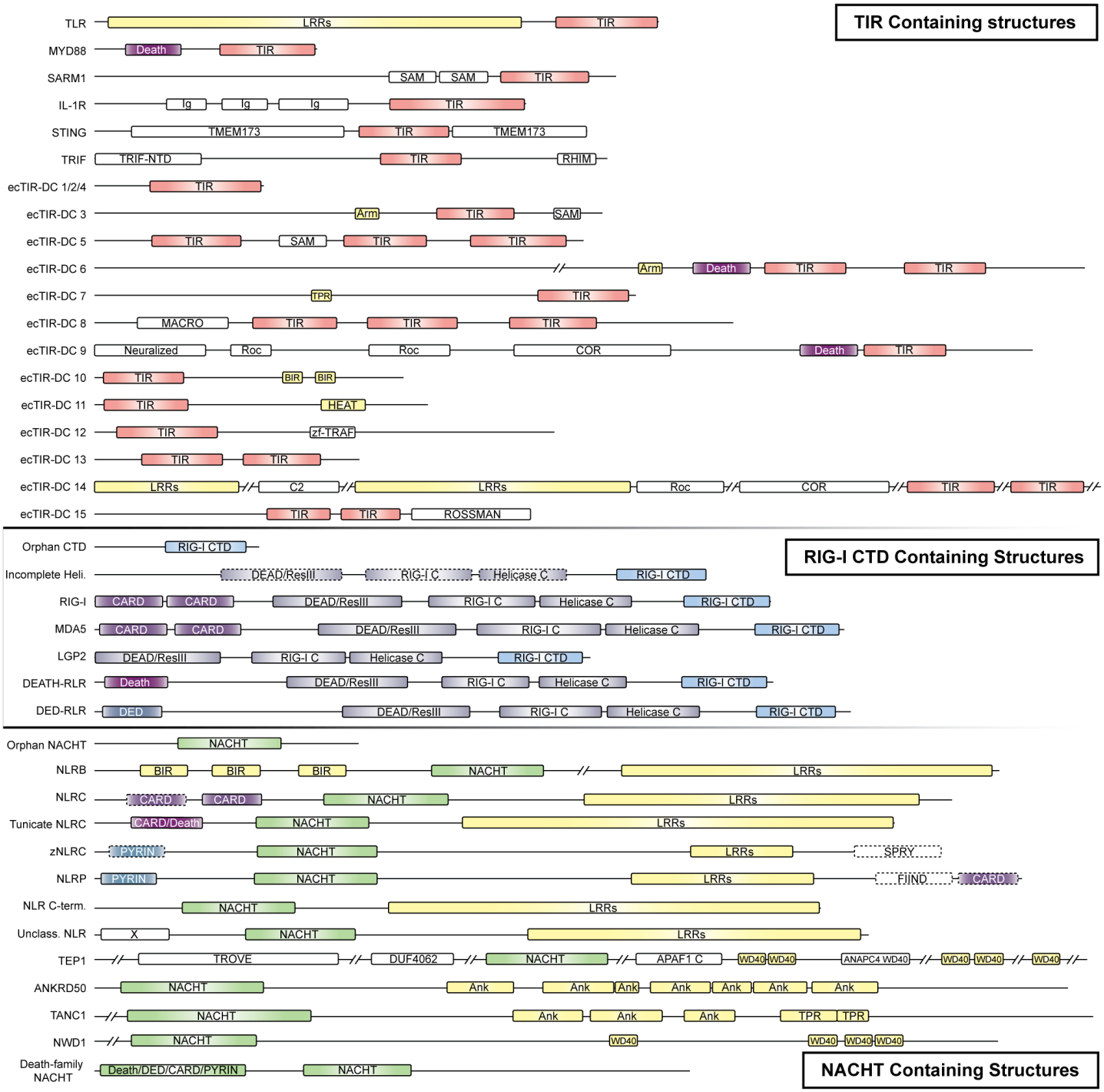

Supplementary Fig 7. Domain architectures associated TIR, RLR C-terminal domain, and NACHT domain revision. Dotted outlines denote domains which are not necessary for protein classification, though may be present.

Hemichordates & Cephalochordates
Strongylocentrotus
Strongylocentrotus
Danio, Coelorhynchus, & Mammal NLRC5
Gnathostome C2TA
Capitella
Cephlochordates
Asteroids
Agnatha
Latimeria & Coelorhynchus
Danio
Latimeria
Mammal NLRPs
Gnathostome NLRC3
Latimeria & Coelorhynchus
Danio zNLRs
Crustacea
Hemichordata
Lophotrochozoa
Hemichordata
Branchiostoma, Lingula, & Schizocardium
Ciona
Schizocardium
Echinodermata
Sarcopterygian NLRC4
Sarcopterygian NLRBs
Amphimedon
Asteroids & Cephalochordates
Vertebrate NOD1/2
0.5

Supplementary Fig 8. Summarized topology of maximum-likelihood phylogenetic reconstruction of all proteins containing both NACHT domains and LRRs using IQ-TREE. All nodes possess ultrafast-bootstrap support ≥95%. Best-fit substitution model by BIC: VT+R10. Scale bar in number of substitutions per site.

Deuterostome RIG-I
LGP2/MDA5
Invertebrate DED-RLR
Asteroidea
S. purpuratus
Echinoidea
S. purpuratus
Hemichordata
Cephalochordata
Acanthaster
Apostichopus
Vertebrata
Crassostrea
Capitella
Helobdella
Notospermus
Lingula
P. australis
Notospermus
Vertebrate LGP2
Vertebrate MDA5
Hemichordata
Cephalochordata
Hemichordata
Lingula
B. belcheri
Nematostella
Schmidtea
Asteroidea
Echinoidea
Cephalochordata
Hemichordata
Lingula
P. australis
Botryllus
Amphimedon
C. elegans
O. vulgaris
Aplysia
Crassostrea
L. anatina
C. elegans
Botryllus
Ciona
Reverse Helicases
Dicer Outgroup
0.2

Supplementary Fig 9. Summarized topology of Bayesian RLR phylogenetic reconstruction. Bold branches mark RLRs identified only after domain revision. Nodes with posterior probabilities (PP) <90% are collapsed. Nodes 90≤PP<100% are marked with white circles. Nodes with 100% PP are marked with black circles. Best-fit substitution model by BIC: VT+F+G. Scale bar in number of substitutions per site.